J|A|C|S
ARTICLES

Published on Web 10/07/2009

Nanoassembled Capsules as Delivery Vehicles for Large Payloads of High Relaxivity Gd^{3+} Agents

Sally E. Plush,[†] Mark Woods,[*,‡,§] You-Fu Zhou,[||] Shyam B. Kadali,[⊥] Michael S. Wong,[⊥,#] and A. Dean Sherry[*,†,||]

Advanced Imaging Research Center, University of Texas Southwestern Medical Center, 5325 Harry Hines Boulevard, Dallas, Texas 75235, Department of Chemistry, Portland State University, P.O. Box 751, Portland, Oregon 97207, Advanced Imaging Research Center, Oregon Health and Sciences University, 3181 S.W. Sam Jackson Park Road, L452, Portland, Oregon 97239, Department of Chemistry, University of Texas at Dallas, P.O. Box 830668, Richardson, Texas, 75083, and Departments of Chemical and Biomolecular Engineering and of Chemistry, Rice University, 6100 Main Street, Houston, Texas 77005

Received August 17, 2009; E-mail: mark.woods@pdx.edu; dean.sherry@utsouthwestern.edu

Abstract: Nanoassembled capsules (NACs) that incorporate a polymer aggregate inside a silica shell may be loaded with agents that are of particular interest for therapeutic or diagnostic applications. NACs formed using the MRI contrast agent $GdDOTP^{5-}$ in the internal polymer aggregate are reported herein, the smaller of which show promise as potential MRI contrast agents. Unlike many other nanoencapsulated systems, water access to the inner core of these NACs does not appear to be limited and consequently the water relaxivity per Gd^{3+} agent can reach as high as 24 mM^{-1} s^{-1}. Robust, spherical capsules were formed using polyallylamine or poly-L-lysine ranging from 0.2 to 5 μm in diameter. The greatest gains in relaxivity were observed for smaller NACs, for which water accessibility remained high but molecular rotation of the Gd^{3+} chelate was effectively restricted. Larger NACs did not afford such large gains in relaxivity, the result of poorer water accessibility combined with less-effective rotational restriction.

Introduction

Magnetic resonance imaging (MRI) is one of the most widely used techniques in clinical medicine. Paramagnetic contrast agents (CAs), usually based on Gd^{3+} complexes, are often administered to increase tissue contrast by accelerating the longitudinal (R_1) relaxation rates of solvent nuclei. The effectiveness of a CA is measured in terms of its relaxivity, the increase in R_1 induced by a 1 mM concentration of the agent. Relaxivity can be broken down into three contributions related to the inner-, second-, and outer-hydration spheres.[1−4] The outer-sphere relaxivity is usually described by modifications to Freed's equations[5] and arises from the diffusion of the complex through the solvent. The relaxivity of the second- and inner-hydration spheres are typically well-described by Solomon, Bloembergen, and Morgan (SBM) theory.[6−10] This indicates that the contribution to relaxivity from these two hydration spheres is determined by a number of parameters including the number and position of the water molecules in each hydration sphere, the rate of exchange of these water molecules with bulk water, the electronic relaxation time of the metal ion, and the rotational correlation time, τ_R, of the complex.[2,3] τ_R increases as the molecular weight of the CA increases, and it has been widely demonstrated that relaxivity can be increased by either covalent or noncovalent association of Gd^{3+} complexes to a slower tumbling macromolecule.[11−17] Although research often focuses upon maximizing inner-sphere relaxivity, the second-hydration

[†] University of Texas Southwestern Medical Center.
[‡] Portland State University.
[§] Oregon Health and Sciences University.
[||] University of Texas at Dallas.
[⊥] Department of Chemical and Biomolecular Engineering, Rice University.
[#] Department of Chemistry, Rice University.

(1) Aime, S.; Botta, M.; Crich, S. G.; Giovenzana, G. B.; Pagliarin, R.; Piccinini, M.; Sisti, M.; Terreno, E. *J. Biol. Inorg. Chem.* **1997**, *2* (4), 470–479.
(2) Aime, S.; Botta, M.; Fasano, M.; Terreno, E. *Chem. Soc. Rev.* **1998**, *27* (1), 19–29.
(3) Caravan, P.; Ellison, J. J.; McMurry, T. J.; Lauffer, R. B. *Chem. Rev.* **1999**, *99* (9), 2293–2352.
(4) Lauffer, R. B. *Chem. Rev.* **1987**, *87* (5), 901–27.
(5) Freed, J. H. *J. Chem. Phys.* **1978**, *68* (9), 4034–4037.
(6) Bloembergen, N. *J. Chem. Phys.* **1957**, *27*, 572–3.
(7) Bloembergen, N.; Morgan, L. O. *J. Chem. Phys.* **1961**, *34*, 842–50.
(8) Bloembergen, N.; Purcell, E. M.; Pound, R. V. *Phys. Rev.* **1948**, *73*, 679–712.
(9) Solomon, I. *Phys. Rev.* **1955**, *99*, 559–65.
(10) Solomon, I.; Bloembergen, N. *J. Chem. Phys.* **1956**, *25*, 261–6.
(11) Glogard, C.; Stensrud, G.; Aime, S. *Magn. Reson. Chem.* **2003**, *41* (8), 585–588.
(12) Nakamura, E.; Makino, K.; Okano, T.; Yamamoto, T.; Yokoyama, M. *J. Controlled Release* **2006**, *114* (3), 325–333.
(13) Nasongkla, N.; Bey, E.; Ren, J.; Ai, H.; Khemtong, C.; Guthi, J. S.; Chin, S.-F.; Sherry, A. D.; Boothman, D. A.; Gao, J. *Nano Lett.* **2006**, *6* (11), 2427–2430.
(14) Rudovsky, J.; Hermann, P.; Botta, M.; Aime, S.; Lukes, I. *Chem. Commun.* **2005**, *20* (18), 2390–2392.
(15) Vaccaro, M.; Accardo, A.; Tesauro, D.; Mangiapia, G.; Loef, D.; Schillen, K.; Soederman, O.; Morelli, G.; Paduano, L. *Langmuir* **2006**, *22* (15), 6635–6643.
(16) Voisin, P.; Ribot, E. J.; Miraux, S.; Bouzier-Sore, A.-K.; Lahitte, J.-F.; Bouchaud, V.; Mornet, S.; Thiaudiere, E.; Franconi, J.-M.; Raison, L.; Labrugere, C.; Delville, M.-H. *Bioconjugate Chem.* **2007**, *18* (4), 1053–1063.
(17) Zhou, Z.; Guo, J.; Yu, H.; Zhu, B.; Liu, C.; Jiang, X.; Zhang, M.; Chen, J. *J. Magn. Reson. Imag.* **2005**, *22* (3), 361–7.

 10.1021/ja906981w CCC: $40.75

and outer-hydration spheres can contribute significantly to the relaxivity of multidentate Gd^{3+} chelates.[4] Although it is difficult to define the number, position, and residence lifetime of water molecules in the second-hydration sphere, and therefore the magnitude of the second-sphere relaxivity, second-sphere contributions can exceed those of the inner-sphere. One such example is $GdDOTP^{5-}$ which, despite having no inner-hydration sphere, has a surprisingly high relaxivity for a molecule with only second-sphere and outer-sphere contributions.[1] It has been shown that phosphonate groups of $GdDOTP^{5-}$ associate with a large number of water molecules in a second-hydration sphere that, in conjunction with the outer-sphere contribution, more than compensates for the absence of an inner-hydration sphere.[18]

The past few years have witnessed an explosion in the use of nanomaterials in drug delivery and molecular imaging. Nanoparticles (NPs) offer a unique platform for combining therapeutic agents and diagnostic imaging capabilities.[19] Many NPs, with their hydrophobic cores and hydrophilic exteriors, are ideal candidates for these combined 'theranostic' agents.[20−22] Furthermore, modification of the particle surface can also result in tissue specific targeting[16] and site specific delivery.[23] In particular NP-based MR contrast agents have found widespread utility for imaging of inflammation,[24,25] a key marker of many pathologies. Recently, we reported the preparation of nanoparticle-assembled capsules (NACs)[26,27] as carriers for drugs via a two-step self-assembly process involving aggregation of the NAC core followed by encapsulation. Aggregation is a charge driven process involving a cationic polymer and a multivalent anion, such as citrate or EDTA, to form an ionically cross-linked polymer−salt aggregate. Small, negatively charged SiO_2 NPs (SiO_2-NPs) when added to a polymer aggregate form a silica shell around the aggregate, stabilizing the capsule.[26−29] Both aggregation and encapsulation occur rapidly at room temperature, in contrast to the layer-by-layer assembly technique, which requires a number of time-consuming steps.[30−33]

In addition to its potential utility as a CA, $GdDOTP^{5-}$ is a multivalent anion that might be used to initiate the charge-driven formation of polymer aggregates in the synthesis of NACs. This approach would allow high levels of capsule loading and potentially lead to an increase in relaxivity.[4] The association of $GdDOTP^{5-}$ with a cationic polymer in the aggregate would be expected to limit the freedom of motion of the chelate so,

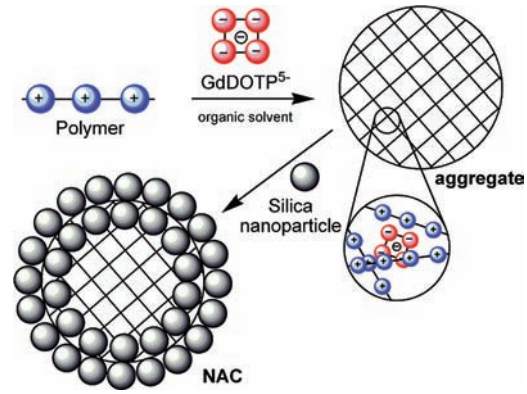

Figure 1. Schematic representation of the synthesis of NACs that encapsulate $GdDOTP^{5-}$.

providing that water molecules have continued access to the second-hydration sphere, the increased rigidity afforded by the aggregate should result in a longer τ_R and higher relaxivities. In addition to controlling the rigidity of the system, and thus the motion of the CA, when designing NP systems for MRI one must ensure that water molecules associated with the CA have access to bulk water as this is critical to the function of an MRI CA.[34,35] Aggregate coatings formed from distinct SiO_2-NPs are known to be permeable to small molecules such as water and should allow access of water to an encapsulated MRI CA.[27,36]

To test this hypothesis, we prepared a series of NACs using $GdDOTP^{5-}$ as an anionic cross-linking reagent (Figure 1). Different cationic polymers, polyallylamine (PAH), poly-L-arginine (PARG), poly-L-lysine (PLL), and fluorescein isothiocyanate tagged polylysine (FITC-PLL), were evaluated to test the general utility of the method. Both PAH and PLL have been used extensively as model cationic polymers to fabricate polyionic complexes,[37,38] and silica NPs exhibit good selectivity and low cytotoxicity, possess good tissue clearance properties, and can be tailored to the meet the requirements of the biological system.[16,39]

Results

NAC Synthesis. The initial step in the formation of the NAC involves mixing a multivalent anion with a cationic polymer to form an aggregate. Previous examples of doped NACs have involved the addition of an agent to a preformed aggregate

(18) Chan, K. W.-Y.; Wong, W.-T. *Coord. Chem. Rev.* **2007**, *251* (17−20), 2428–2451.
(19) Wickline, S. A.; Lanza, G. M. *J. Cell. Biochem.* **2002**, *Suppl. 39*, 90–97.
(20) Kwon, G. S. *Crit. Rev. Ther. Drug Carrier Syst.* **2003**, *20* (5), 357–403.
(21) Otsuka, H.; Nagasaki, Y.; Kataoka, K. *Adv. Drug Delivery Rev.* **2003**, *55* (3), 403–419.
(22) Torchilin, V. P. *J. Controlled Release* **2001**, *73* (2−3), 137–172.
(23) Santra, S.; Bagwe, R. P.; Dutta, D.; Stanley, J. T.; Walter, G. A.; Tan, W.; Moudgil, B. M.; Mericle, R. A. *Adv. Mater.* **2005**, *17* (18), 2165–2169.
(24) Petry, K. G.; Boiziau, C.; Dousset, V.; Brochet, B. *Neurotherapeutics* **2007**, *4* (3), 434–442.
(25) Corot, C.; Petry, K. G.; Trivedi, R.; Saleh, A.; Jonkmanns, C.; Le Bas, J.-F.; Blezer, E.; Rausch, M.; Brochet, B.; Foster-Gareau, P.; Baleriaux, D.; Gaillard, S.; Dousset, V. *Invest. Radiol.* **2004**, *39* (10), 619–625.
(26) Murthy, V. S.; Rana, R. K.; Wong, M. S. *J. Phys. Chem. B* **2006**, *110* (51), 25619–25627.
(27) Rana, R. K.; Murphy, V. S.; Yu, J.; Wong, M. S. *Adv. Mater.* **2005**, *17* (9), 1145–1150.
(28) Kadali, S. B.; Soultanidis, N.; Wong, M. S. *Top. Catal.* **2008**, *49* (3−4), 251–258.
(29) Yu, J.; Murthy, V. S.; Rana, R. K.; Wong, M. S. *Chem. Commun.* **2006**, *21* (10), 1097–1099.
(30) Caruso, F. *Chem.—Eur. J.* **2000**, *6* (3), 413–419.
(31) Caruso, F.; Caruso, R. A.; Moehwald, H. *Science* **1998**, *282* (5391), 1111–1114.
(32) Cha, J. N.; Birkedal, H.; Euliss, L. E.; Bartl, M. H.; Wong, M. S.; Deming, T. J.; Stucky, G. D. *J. Am. Chem. Soc.* **2003**, *125* (27), 8285–8289.
(33) Murthy, V. S.; Cha, J. N.; Stucky, G. D.; Wong, M. S. *J. Am. Chem. Soc.* **2004**, *126* (16), 5292–5299.
(34) Koenig, S. H.; Ahkong, Q. F.; Brown, R. D., III; Lafleur, M.; Spiller, M.; Unger, E.; Tilcock, C. *Magn. Reson. Med.* **1992**, *23* (2), 275–86.
(35) Reynolds, C. H.; Annan, N.; Beshah, K.; Huber, J. H.; Shaber, S. H.; Lenkinski, R. E.; Wortman, J. A. *J. Am. Chem. Soc.* **2000**, *122* (37), 8940–8945.
(36) Muñoz Tavera, E.; Kadali, S. B.; Bagaria, H. G.; Liu, A. W.; Wong, M. S. *AIChE J.* **2009**, *55* (11), 2950–2965.
(37) Dai, Z.; Voigt, A.; Leporatti, S.; Donath, E.; Dahne, L.; Mohwald, H. *Adv. Mater.* **2001**, *13* (17), 1339–1342.
(38) Na, K.; Kim, S.; Park, K.; Kim, K.; Woo, D. G.; Kwon, I. C.; Chung, H.-M.; Park, K.-H. *J. Am. Chem. Soc.* **2007**, *129* (18), 5788–5789.
(39) Kneuer, C.; Sameti, M.; Bakowsky, U.; Schiestel, T.; Schirra, H.; Schmidt, H.; Lehr, C.-M. *Bioconjugate Chem.* **2000**, *11* (6), 926–932.

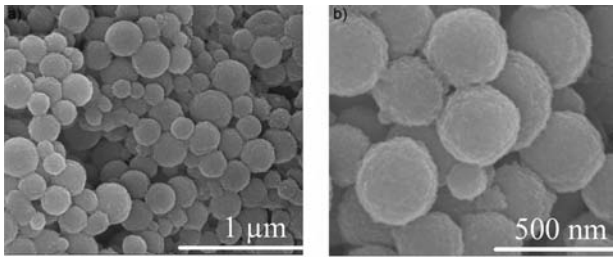

Figure 2. SEM images of PAH-based NACs ($R = 0.5$) prepared in 2:1 $EtOH/H_2O$.

consisting of a simple anion, such as citrate or EDTA mixed with PAH.[26,27] Given the multivalency of $GdDOTP^{5-}$, we reasoned that the complex itself could be used as the aggregation agent, eliminating the need for an additional cross-linking anion. Aggregates were prepared by mixing a solution of $GdDOTP^{5-}$ with a cationic polymer after which the solution became turbid.[27] Initial attempts to form aggregates between $GdDOTP^{5-}$ and PAH or PLL in water were unsuccessful. However, it was found that by switching to mixed aqueous/organic solvent systems that aggregation could be achieved and stable NACs could be synthesized at room temperature. PAH-based aggregates formed in solutions of either 2:1 $EtOH/H_2O$ or 1:1 CH_3CN/H_2O depending on the desired ratio of polymer to anion, but PLL-based aggregates could only be synthesized in 1:1 CH_3CN/H_2O. Interestingly, when PARG was mixed with $GdDOTP^{5-}$ in H_2O, the solution became turbid almost immediately suggesting the formation of an aggregate with ion-pair interactions that differ from those found in the PLL and PAH system.

The aggregate can then be stabilized by encapsulation with SiO_2-NPs which provide a stable outer shell which, it is anticipated, will also be biocompatible. Encapsulation of the aggregates was performed by adding a 2% solution of SiO_2-NP (13 nm diameter) to the CA−polymer aggregate suspension and thoroughly mixing the solution. The turbidity of the solution increased further upon addition of the SiO_2-NPs. Particles were prepared at a specific charge ratio, R, defined as the ratio of total negative charge of the anion to the total positive charge of the polymer (eq 1).

$$R = \frac{[\text{anion}]_{\text{final}} \times |z-|}{[\text{polymer}]_{\text{final}} \times |z+|} \quad (1)$$

where $z-$ is the negative charge per anion and $z+$ is the positive charge per chain.[26] PAH- and PARG-based NACs were prepared with R ratios of 0.5, 1.0, 2.5, and 5.0; PLL-based NACs were prepared with R ratios of 0.25, 0.5, 1.0, 2.5, and 5.0. Solutions of the NACs were filtered through 10kD MWCO membranes, and analysis of the filtrate for Gd^{3+} by ICP-MS showed that level of Gd^{3+} in the filtrate was below the detection limits of ICP, indicating that essentially all the $GdDOTP^{5-}$ was trapped within the NAC core. Figure 2 shows SEM images of PAH-based NACs ($R = 0.5$), the elemental composition of which were confirmed by EDAX (Supplementary Figure S1).

In general, the NACs formed using PAH and PLL polymer constructs appeared spherical in shape, with diameters ranging from 200 nm to 5 μm, depending upon the R ratio employed (Table 1), and appeared to be structurally robust. In contrast the PARG-based NACs were neither as robust nor as uniform; NAC morphology could not be improved by either altering the solvent system or changing the R value (Supplementary Figure S2).

Table 1. Capsule Diameters (μm), from DLS, and Relaxivities, r_1 (23 MHz, 25°C), of $GdDOTP^{5-}$-Based NACs As a Function of Anion to Polymer Ratio (R)

	capsule diameter (μm)				
	$R = 0.25$	$R = 0.5$	$R = 1$	$R = 2.5$	$R = 5$
PAH (2:1 $EtOH/H_2O$)	nf[a]	0.5	1.2	2.8	4.5
PAH (1:1 CH_3CN/H_2O)	nf	0.2	0.2	0.5	nf
PLL (1:1 CH_3CN/H_2O)	0.8	1.8	2.3	3.1	>4.5
FITC-PLL (1:1 CH_3CN/H_2O)	nf	0.26	0.3	0.8	1.0
	relaxivity (mM^{-1} s^{-1})				
PAH (2:1 $EtOH/H_2O$)	nf	23.98	20.33	10.97	8.51
PAH (1:1 CH_3CN/H_2O)	nf	24.17	22.80	11.94	nf
PLL (1:1 CH_3CN/H_2O)	23.02	11.10	6.25	4.40	3.73
FITC-PLL (1:1 CH_3CN/H_2O)	nf	9.78	6.22	5.27	4.60

[a] nf = NACs were not formed.

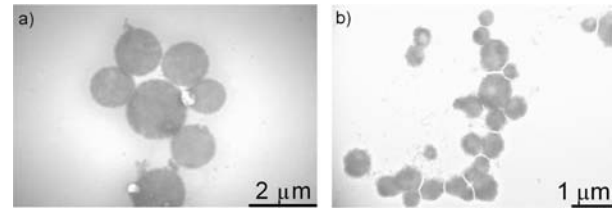

Figure 3. TEM images of PAH-based NACs ($R = 2.5$) prepared in (a) 2:1 $EtOH/H_2O$ and (b) 1:1 CH_3CN/H_2O.

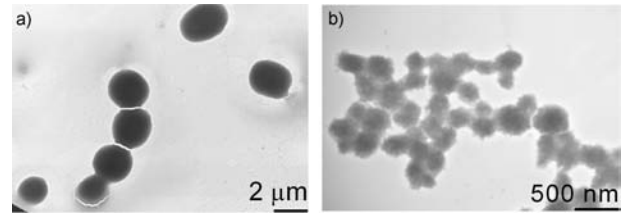

Figure 4. TEM images of (a) PLL-based NACs ($R = 1$) and (b) FITC-PLL-based NACs ($R = 1$), 1:1 CH_3CN/H_2O.

The particle size, determined by DLS and TEM, was found to be highly dependent on the concentration of $GdDOTP^{5-}$ (Table 1). As the ratio of anion to polymer increases, the particle size was observed to increase for both the PLL- and PAH-based NACs, although this change was more pronounced for the PLL-based NACs. The solvent in which PAH-based NACs were prepared also strongly influences NAC size (Figure 3 and Table 1); as the dielectric constant of the solvent system was decreased, so the size of the particles also decreased. Interestingly, when PLL is replaced with FITC-tagged PLL in the aggregation step, the resulting NACs were smaller (Figure 4 and Table 1). TEM images of other NAC systems are shown in Supplementary Figures S3−S6. Flow cytometry was used to determine the average number of NACs synthesized for each R ratio in an attempt to determine the amount of Gd^{3+} per particle. In general, the smaller the NAC the higher the counts, indicating that a greater number of NACs formed when lower R ratios are employed. From the cell counts, it was determined that each NAC contains only picomolar quantities of $GdDOTP^{5-}$ with smaller NACs containing less Gd^{3+} chelate per capsule.

Relaxometric Studies. It was anticipated that the changes in capsule morphology arising from the different polymers and R ratios would also result in differences in the relaxivity of the $GdDOTP^{5-}$ held within the NACs. The relaxivity per Gd^{3+} of each NAC was measured by recording the longitudinal relaxation rate ($1/T_1$) of aqueous solutions of the CA at different concentrations. Since ICP-MS showed that all the $GdDOTP^{5-}$

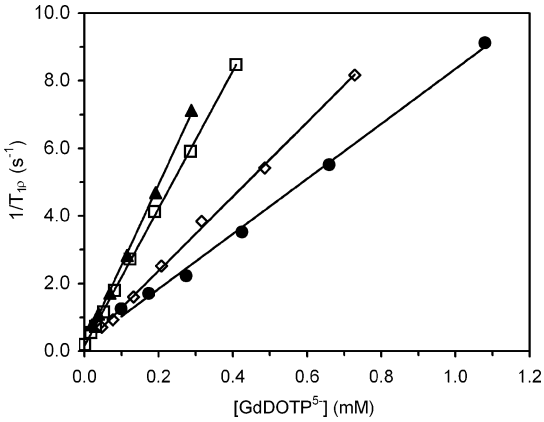

Figure 5. Experimentally measured longitudinal relaxation rates ($1/T_{1\rho}$) for PAH-based NACs prepared in 2:1 EtOH/H_2O; $R = 0.5$ (▲), $R = 1$ (□), $R = 2.5$ (◇), and $R = 5$ (●). [$GdDOTP^{5-}$] indicates the *total* concentration of $GdDOTP^{5-}$. Regressions show a goodness of fit of $R^2 > 0.998$. See Supplementary Figures S8, S9, and S10 for other NACs.

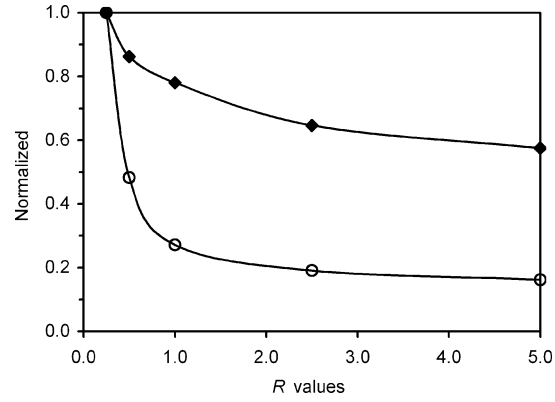

Figure 6. Change in the normalized r_1 (□) and Fp (◆) (normalized to the maximum observed value) as a function of NAC *R* ratio for PLL-FTIC/$GdDOTP^{5-}$ NACs.

was either encapsulated or at least tightly associated with the NAC, any contribution to overall relaxivity from free $GdDOTP^{5-}$ could be neglected and the concentration of Gd^{3+} was calculated from the quantity of $GdDOTP^{5-}$ employed in the NAC synthesis and confirmed by ICP-MS. The relaxivity was then determined by linear regression analysis. It is noteworthy that the $1/T_1$ measured for solutions of the diamagnetic SiO_2-NP did not differ significantly from that of water indicating that the particles themselves do not contribute to relaxivity. The concentration dependence of $1/T_1$ was linear for all NACs (Figure 6 and Supplementary Figures S8, S9, and S10); relaxivity values are reported in Table 1.

Figure 5 illustrates the substantial changes in relaxivity that arise from changing the *R* ratio in PAH-based NACs. In most cases, the relaxivity is enhanced relative to $GdDOTP^{5-}$ ($r_1 = 4.9\ mM^{-1}\ s^{-1}$), but it is enhanced most when the value of *R* is smaller; an impressive >4-fold enhancement was observed for NACs with $R \leq 1$. Inspection of Table 1 shows the trend of higher relaxivity enhancements with lower *R* ratios was observed for all NACs regardless of the polymer or solvent system used during the synthesis. Notably once particles exceed a certain size (PLL (1:1 CH_3CN/H_2O) $R = 5$, diameter >4.5 μm) then the effect of encapsulating $GdDOTP^{5-}$ is to reduce rather than enhance the relaxivity of the $GdDOTP^{5-}$ chelate (Table 1).

Since relaxivity is inherently linked to the extent of molecular motion, the freedom of motion available to components of the aggregate core was of interest. Fluorescence polarization (Fp) measurements can afford insight into these local molecular motions by measuring the ratio of emission intensities parallel and perpendicular to the plane of linearly polarized excitation light. A greater freedom of motion is reflected in smaller fluorescence polarization ratios. To ascertain the difference in Fp across an NAC series and gain further insight into how the value of *R* affects the τ_R of the $GdDOTP^{5-}$, NACs with different *R* ratios were prepared using FTIC-tagged PLL. The fluorescence intensities of the FITC groups were then measured parallel and perpendicular to the excitation plane. The magnitude of the fluorescence polarization was found to be much larger for smaller NACs (low *R* ratio) than for larger NACs (high *R* ratio). The Fp measurements were then compared to the relaxivity results by normalizing each to the maximum experimentally obtained value for each parameter and plotting them both as a function of the NAC R ratio (Figure 6).

Discussion

Three factors appear to govern whether or not NACs can be produced and the nature of those NACs when the potential MRI CA $GdDOTP^{5-}$ is employed as the anion in the aggregation step: the nature of the cationic polymer, the charge ratio *R*, and the nature of the solvent system. PARG was the only cationic polymer tested that would aggregate with $GdDOTP^{5-}$ in aqueous solution. Aggregates could only form in mixed aqueous/organic solvents in the cases of PLL and PAH. Presumably introducing an organic solvent diminishes the charge stabilizing capacity of the solvent thereby increasing the Coulombic interaction between the anion and cationic polymer and favoring aggregation. These results suggest that the nature or extent of the interaction between the $GdDOTP^{5-}$ anion and the guanidine groups of PARG is different from that of the primary amines of PLL or PAH. A difference in the nature of the interaction may also have a profound effect upon the success of the subsequent encapsulation procedure. When aggregates formed with the primary amine based systems, PLL and PAH, were treated with SiO_2-NPs, NACs formed that were spherical and robust (TEM images taken three weeks after synthesis showed very little deformity); NACs derived from PARG possessed neither of these qualities. Indeed, PARG-based NACs were of such poor quality that further study was not undertaken.

Controlling the size of the NAC is extremely important for *in vivo* applications. The formation of smaller, submicrometer NACs increases the potential utility of these constructs in biological systems. From the results presented above, it is clear that, by careful selection of the polymer and solvent system used in the aggregation step, the NAC size and quantity of CA contained therein can be accurately controlled over a fairly large range. The smallest particles (~200 nm diameter) are obtained when PAH is used in 1:1 CH_3CN/H_2O solvent mixtures. Changing the solvent to the more protic 1:1 EtOH/H_2O mixture, or the polymer to PLL, leads to substantial increases in particle size, although notably the latter has a significantly more profound effect. The charge ratio *R* employed also has a considerable effect on the resulting NAC size: larger *R* ratios leading to larger NACs, a trend observed across all polymers and solvent systems. The very largest particles (~5 μm diameter) are obtained when PLL at $R = 5$ is used in CH_3CN/H_2O mixtures. Notably when the large aromatic component, FTIC,

was incorporated into PLL, the NACs are approximately an order of magnitude smaller than those obtained than with PLL under otherwise identical conditions. Submicrometer sized NACs (diameter 200−300 nm) are reliably afforded by using PAH or FITC-PLL in 1:1 CH_3CN/H_2O with $R \leq 1$.

$GdDOTP^{5-}$ is a more charge dense anion than EDTA or citrate,[26,27] and this may affect the interaction with the cationic groups of different polymers. Differences in the spacing and flexibility of the cationic groups of PLL and PAH and the flexibility of the polymer backbone could cause the observed differences in NAC size. The extent to which a polymer coils in solution and the tightness of those coils are highly dependent upon solvation.[40] Thus, we may reasonably expect that solvents that promote more, tighter polymer coils would lead to more compact aggregates and smaller NACs. These factors may also account for the different range of R ratios over which NACs could be formed for the two polymer systems. It seems highly likely that the interior of an NAC will vary considerably depending upon how, and from which polymer, it was prepared; these differences have important implications for the relaxivity of the encapsulated $GdDOTP^{5-}$ as can be seen from the measured relaxivities values.

For NACs to be useful as contrast media for MRI, it is vital that water can exchange between the core structure and the bulk. In order for the encapsulated $GdDOTP^{5-}$ to catalyze the relaxation of solvent water protons, the solvent water must also be free to enter the second-hydration sphere of the complex. It is now well established that the silica coating of these NACs are permeable to small molecules such as water,[27,36] and in this case this permeability was confirmed by examining the diffusion of FTIC-tagged dextrans into the inner core using confocal microscopy (Supplementary Figure S7). This is further supported by the observation of enhanced relaxivities observed for most NACs, something that can only occur if water is able to freely access the second hydration sphere of $GdDOTP^{5-}$. The temperature dependence of relaxivity can provide insights into the exchange processes that dominate in systems such as this. The relaxivity of PAH- and PLL-based NACs increase slightly with decreasing temperature; a similar trend is observed for $GdDOTP^{5-}$ (Supplementary Figures S11 and S12). These temperature profiles are consistent with fast water exchange kinetics for all four NAC systems, and the similarity of these temperature profiles indicates that water access to the ion-paired $GdDOTP^{5-}$ CA is not compromised significantly by encapsulation within the NAC. Thus we can conclude that not only is water able to freely access $GdDOTP^{5-}$ within the NAC, but the chelate retains the rapid exchange kinetics required for high relaxivity.

The 4−5-fold relaxivity enhancement (with r_1 reaching as much as 24 mM^{-1} s^{-1}) observed for the smallest NACs is consistent with the Fp measurements from the FTIC-tagged PLL experiments that indicate restricted molecular reorientation within the aggregate core. The longer τ_R of $GdDOTP^{5-}$ when encapsulated in an NAC leads to higher relaxivity. As NAC size increases, the relaxivity per Gd^{3+} drops off. This trend was also mirrored in the Fp experiments, indicating a greater freedom of motion and, hence, shorter τ_R as the NAC size increases. A number of other types of nanomaterials have also shown relaxivity enhancements with decreasing size and been attributed to changes in τ_R.[41,42] However, the accessibility of $GdDOTP^{5-}$ to water would be expected to diminish as the NAC size increases. At low R ratios the chelate is not denied access to water, but as the size of the NAC also increases so must the average distance a water molecule must travel from a chelate to reach the bulk water. It appears that this scenario becomes particularly acute in the case of the largest PLL-based NACs ($R = 5$) for which the relaxivity of Gd^{3+} is lower than that of $GdDOTP^{5-}$ itself. This phenomenon cannot be the result of ineffective restriction of molecular motion alone; there must also exist inhibition of the movement of water in these larger NACs. If second-sphere water molecules of chelates buried at the center of a large NACs were unable to find their way rapidly into the bulk solvent, then this would limit relaxivity as observed for the largest NACs. Given the preference for small particle sizes for in vivo applications, and the substantial relaxivity gains observed for smaller NACs, the use of small R ratios to provide small NACs with high relaxivities could provide a method for more effective MR imaging agents.

Conclusions

$GdDOTP^{5-}$ can be used as the basis for the formation of silica-shelled NACs, facilitating the incorporation of MRI contrast media into the NAC core. This approach has several advantages: incorporating $GdDOTP^{5-}$ within the aggregate core restricts the molecular rotation of the contrast agent leading to relaxivity enhancement; the silica shell employed not only is tolerated in vivo but is also permeable to water allowing the $GdDOTP^{5-}$ to function in its role as a T_1-shortening agent; the size and properties of the NAC can be carefully controlled during synthesis by appropriate selection of the cationic polymer, the solvent system, and the R charge ratio. By encapsulating Gd^{3+} within the NAC, we are able to not only increase the relaxivity of each individual Gd^{3+} ion but also construct an agent in which large quantities of high relaxivity Gd^{3+} are delivered. This has implications for the field of targeted MR imaging in which iron oxide based nanoparticles are often used to generate large changes in MR signal from low concentrations of agents. However, by employing a high payload of T_1-shortening Gd^{3+}, rather than the T_2- or often T_2*-shortening iron oxide, we potentially open the door to the quantification of targeted imaging, something that is hard to achieve with T_2- or T_2*-weighted imaging sequences.

Experimental Section

General Remarks. Poly(allylamine hydrochloride) (PAH, 70,000 g/mol), poly-L-arginine (50,000 g/mol), poly-L-lysine (50 000 g/mol), fluorescein isothiocyanate tagged poly-L-lysine (FTIC-PLL, MW = 30−70 kD, 0.003−0.01 mol of FITC per mol) were purchased from the Sigma-Aldrich company and used as received. $GdDOTP^{5-}$ was synthesized according to previously reported procedures.[43] SiO_2-NPs were purchased as an aqueous colloidal suspension (13 nm diameter, 20.5 wt %, pH 3.4) from Snowtex-O, Nissan Chemicals and were used without further purification. All solutions were prepared using particle-free deionized water. A concentrated solution of $GdDOTP^{5-}$ was initially prepared in pure

(40) Rubinstein, M.; Colby, R. H. *Polymer Physics*; Oxford University Press: Oxford, 2007; Chapter 5.

(41) Na, H. B.; Lee, J. H.; An, K.; Park, Y. I.; Park, M.; Lee, I. S.; Nam, D.-H.; Kim, S. T.; Kim, S.-H.; Kim, S.-W.; Lim, K.-H.; Kim, K.-S.; Kim, S.-O.; Hyeon, T. *Angew. Chem., Int. Ed.* **2007**, *46* (28), 5397–5401.

(42) Su, C.-H.; Sheu, H.-S.; Lin, C.-Y.; Huang, C.-C.; Lo, Y.-W.; Pu, Y.-C.; Weng, J.-C.; Shieh, D.-B.; Chen, J.-H.; Yeh, C.-S. *J. Am. Chem. Soc.* **2007**, *129* (7), 2139–46.

(43) Geraldes, C. F. G. C.; Sherry, A. D.; Kiefer, G. E. *J. Magn. Reson.* **1992**, *97* (2), 290–304.

H_2O and then diluted with the appropriate solvent system required for particle synthesis.

Synthesis. Polymer solutions (20 μL, 0.071 M) in pure H_2O, 2:1 EtOH/H_2O, or 1:1 CH_3CN/H_2O (*v*/*v*) were added to a stock solution of $GdDOTP^{5-}$ (120 μL) in the same solvent at pH $\geq$ 9. The charge ratio *R* was varied by varying the initial concentration of $GdDOTP^{5-}$. Immediately upon mixing, the solutions became turbid reflecting formation of polymer−anion aggregates. The solution was vortexed at low speed for 10 s and then aged for 10 min. After aging, a 2% SiO_2-NP solution (100 μL) was added, and the resulting suspension was vortexed for 20 s at medium speed to yield the final NACs. Particles were then washed by filtration using a 10 kDMWCO membrane. PAH-based NACs were formed with *R* varying from 0.5 to 5.0 (initial $GdDOTP^{5-}$ stock solutions ranging from 1.2 to 12 mM) in either a 2:1 EtOH/H_2O or 1:1 CH_3CN/H_2O (*v*/*v*) solvent system. PLL-based NACs and FITC-PLL-based NACs were formed varying *R* from 0.25 to 5.0 (initial $GdDOTP^{5-}$ stock solutions ranging from 0.6 to 12 mM) in a 1:1 CH_3CN/H_2O (*v*/*v*) solvent system. All syntheses undertaken in the absence of an organic cosolvent were unsuccessful. PARG-based NACs were formed with *R* varying from 0.5 to 50 (initial $GdDOTP^{5-}$ stock solutions ranging from 1.2 to 12 mM) in 100% H_2O; however these NACs were not robust.

Transmission Electron Microscopy (TEM). TEM imaging was performed on a JEOL 1200 EX system with an accelerating voltage of 40 to 120 Kv and mounted with a Sis Morada 11 mpixel CCD camera. A solution of NACs was cast onto a carbon/copper TEM grid for imaging. The solution was allowed to absorb onto the grid for an average of 5 min followed by removal of excess sample by blotting.

Dynamic Light Scattering (DLS). Size distribution analysis was carried out on a DLS Model 802 (Viscotek, Houston, TX). Scattered light (825 nm) was detected at an angle of 90° at 25 °C in a Hellma quartz ultramicro cell. The sample concentration for measurements was 1.4 mg mL^{-1}. The data for each sample were obtained in five independent measurements.

Relaxometry. NACs were diluted in water affording a solution of initial volume 500 μL. The concentration of $GdDOTP^{5-}$ in the solution at the commencement of the relaxivity measurements varied for each type of NAC, ranging from 0.28 to 2.8 mM for PAH NACs, corresponding to *R* ratios of 1 to 5, and from 0.14 to 2.8 mM for PLL NACs, corresponding to *R* ratios of 0.25 to 5. The T_1 of each NAC suspension was determined using an inversion recovery pulse sequence on an Oxford MARAN Ultra Resonance relaxometer operating at 23 MHz. The sample temperature was controlled by circulating water through the probe using an external water bath and pump. The resulting relaxation decay curves were fitted to a monoexponential function to obtain T_1. All lines were fitted with an $R^2 > 0.998$. Measurements were performed for each particle composition in duplicate. The relaxivity of $GdDOTP^{5-}$ in water was measured at $r_1 = 4.9$ mM^{-1} s^{-1} (23 MHz, 25 °C, pH 6.5).

Flow Cytometry. The NACs were counted using flow cytometry with a BioDistribution FACScan LSR II system. A 30 s run with a flow rate of 24 μL s^{-1} was used in conjunction with a 480 nm laser.

Permeability Measurements. Fluorescein isothiocyanate dextran (FITC-Dextran, Aldrich) with a molecular weight of 4400 was used for permeability test experiments. Typically a 20 μL aliquot of a NAC solution (as synthesized) was mixed with 20 μL of a FITC-Dextran solution on a glass slide placed in a holder of the confocal microscope. The measurements were taken at 10 min intervals after mixing.

Fluorescence Polarization. Fluorescence polarization (Fp) was measured as a ratio of the fluorescence intensity parallel to the excitation plane (FI_{pa}) with respect to the fluorescence intensity perpendicular to the excitation plane (FI_{pe}) (eq 2).

$$\mathrm{Fp} = \frac{(\mathrm{FI_{pa}} - \mathrm{FI_{pe}})}{(\mathrm{FI_{pa}} + \mathrm{FI_{pe}})} \tag{2}$$

NACs were prepared using fluorescein isothiocyanate tagged polylysine (FITC-PLL). Typically, a 20 μL aliquot of a solution of NAC, prepared from FITC-PLL, was diluted into 1 mL, and the fluorescence intensity parallel and perpendicular to the excitation plane were measured.

Acknowledgment. The authors thank the National Institutes of Health (RR-02584, CA-126608, and CA-115531), the Robert A Welch Foundation (AT-584), 3M (NTF Award), the National Science Foundation (CBET-0652073), Portland State University, Oregon Opportunity, and the Kobayashi Graduate Student Fellowship (to S.B.K.) for financial assistance. We also thank both the MCIF and flow cytometry core facilities and Professor Gao's research group at UT Southwestern Medical Center for valuable discussions.

Supporting Information Available: Figures showing: EDAX spectrum of PAH-based NACs; TEM images of PARG-based NACs, PAH-based NACs formed in 2:1 EtOH/H_2O and 1:1 CH_3CN/H_2O, PLL-based NACs and FTIC-PLL-based NACs; Confocal microscopy images of FTIC-PLL-based NACs; relaxivity determinations for all NACs not presented in the text; temperature dependence of the relaxivity of all NACs. This material is available free of charge via the Internet at http://pubs.acs.org.

JA906981W